NuMu Note #166

Emittance Exchange using thick Bent Solenoid elements

R.C. Fernow
Brookhaven National Laboratory

1 September 2000

Abstract

We examine the use of thick bent solenoid elements in 6-dimensional emittance exchange systems. We review the basic properties of bent solenoids and the fundamental design considerations for emittance exchange systems that combine bent solenoids and rf cavities. We discuss the parameter selection for an actual system. As we have been unable to find a satisfactory solution so far, suggestions are given for further research.

1 Introduction

Direct cooling of the longitudinal phase space of a muon beam is very inefficient, so reduction of longitudinal phase space relies instead on emittance exchange [1]. In this process wedge-shaped absorbers in dispersive regions of the magnetic lattice reduce the momentum spread in the beam, while allowing the transverse area of the beam to increase [2]. This represents an exchange of transverse for longitudinal emittance. A bent solenoid produces dispersion in the plane perpendicular to the bend. Since transverse cooling is done in a large acceptance, straight solenoid lattice, it seems natural to try to incorporate bent solenoids in an associated emittance exchange system.

There are two general approaches to the design of a cooling channel incorporating emittance exchange. The approach used in the Status Report [1] and investigated further here is to design a separate emittance exchange system that alternates with pure transverse cooling sections in the cooling channel. This isolates the problem of emittance exchange from constraints imposed by the transverse cooling process, but requires matching sections each time one changes the type of lattice. Alternative approaches, which could very well have better performance, are to introduce thin dispersive elements periodically in a transverse cooling lattice or to design a conductor

configuration that cools transversely and exchanges simultaneously.

The goal for a stand-alone emittance exchange system for a muon collider is to produce a beam with the following properties:

1. the momentum spread should be reduced by a factor of ~0.5
2. the bunch length should approximately equal that of the input beam
3. the transverse area should be symmetric and larger by a factor ~2
4. the transverse divergences should approximately equal that of the input beam
5. the mean momentum should approximately equal that of the input beam

If these requirements are all met, the 6-dimensional invariant emittance of the beam will be conserved and we will have achieved a pure exchange.

In this note we examine stand-alone exchange systems that use "thick" bent solenoid elements, where thick means a longitudinal extent equal to one or more Larmor wavelengths[1]

$$\lambda_L = 2\pi \frac{p_Z}{e\, B_S} \qquad \textbf{(1)}$$

where p_Z is the particle's momentum and B_S is the solenoidal component of the field.

Even for the study of thick bent solenoid elements there is the question of how to represent the bent solenoid fields. For this note we will use exclusively analytic fields derived from a vector potential [3]. Alternatively one can look at bent solenoids built up from current loops following a curved geometric path [4].

Further Research - Compare quantitatively the fields derived from these two approaches.

The current state of the art in emittance exchange design using thick bent solenoids is the 5-D solution by R. Palmer described in the muon collider Status Report [1]. This solution was quite successful in reducing the momentum spread, but ignored serious bunch lengthening effects. Even without the time dimension there was not a clean exchange, since there was a growth of 39% in 5-D emittance. This note builds on the work described in the Status Report to consider exchange systems for all 6 dimensions.

[1] In this and the following equations substitute 0.3 for *e* when using m, GeV/c and T as units.

2 Basic properties of bent solenoids

Particles undergo complicated trajectories inside a bent solenoid. The particles revolve around the local field direction at the cyclotron frequency

$$\omega_C = \frac{e\,B_S}{m\,\gamma} \tag{2}$$

The distance of the particle from the center of revolution in a plane perpendicular to the local field line is

$$r_L = \frac{p_\perp}{e\,B_S} \tag{3}$$

The locus of these centers of revolution is called the *guide ray*.

The interest in bent solenoids comes from the fact that it produces dispersion in the location of the guide ray in the plane perpendicular to the bend [3-7]. The dispersion arises from two sources known as *curvature drift* and *grad B* drift. In the bent solenoid the field lines are curved with more lines concentrated nearer the center of curvature. Curvature drift arises from the centrifugal force felt by particles encountering curved field lines and is proportional to the component of the particle's velocity along the local field direction. Grad B drift comes from the fact that in a non-uniform field the particle sees different local fields on one side of its cyclotron oscillation as the other and is proportional to the component of the particle's velocity perpendicular to the local field direction.

In a pure bent solenoid all particles of a given charge are bent in the same direction by an amount proportional to their momentum. For emittance exchange it is more convenient to have the guide ray for the reference momentum p_0 pass thru undeflected. This can be done by superimposing a dipole magnetic field with strength

$$B_D = \frac{p_0}{e\,R_{bend}} \tag{4}$$

over the bent solenoid. The radius of curvature of the dipole field must equal the radius of curvature of the bent solenoid. The total bend angle of a sector dipole with normal entrance and exit angles is

$$\theta_{bend} = \frac{e}{p_o}\int B_D\,ds \tag{5}$$

With the dipole field present particles with momentum smaller than p_0 are deflected one way, while particles with momentum greater than p_0 are deflected the other. The deflection in the guide ray position is then given by [6]

$$\Delta y_G = \frac{p}{e\,B_S}\,\frac{\Delta p}{p}\,\theta_{bend} \qquad \textbf{(6)}$$

The dispersion is

$$D = \frac{\Delta y_G}{\frac{\Delta p}{p}} = \frac{p}{e\,B_S}\,\theta_{bend} \qquad \textbf{(7)}$$

For the case of a thick element with a length of one Larmor wavelength this can be written as

$$D = 2\pi\,\frac{p_Z}{e}\,\frac{B_D}{B_S^2} \qquad \textbf{(8)}$$

Note that the dispersion drops quadratically as the solenoid field strength is increased.

3 General considerations

Before discussing the design on an actual exchange system let us examine some properties of the various components.

3.1 Orbit dynamics in the bent solenoid field

We start by looking at the particle behavior in a bent solenoid system under the most favorable conditions, in order to see how well the system works in principle. We assume the first order fields in the system of the bent solenoid and compensating dipole are given by

$$\begin{aligned} B_X(x,y,s) &= g_Q\,y \\ B_Y(x,y,s) &= b_D + g_Q\,x \\ B_S(x,y,s) &= b_S\,(1 - h\,x) \end{aligned} \qquad \textbf{(9)}$$

where b_S and b_D are the solenoid and dipole strength respectively and g_Q is the quadrupole gradient. The curvature *h* is given by

$$h = \frac{1}{R_{bend}} = \frac{e}{p_0} b_D \qquad \textbf{(10)}$$

In first order the field strength parameters and the curvature are constants, so the field components do not depend on the longitudinal coordinate *s*. Issues such as coupling or matching must be postponed temporarily since they depend on the longitudinal field shape.

Consider an idealized beam with properties given in Table 1.

Table 1 Ideal beam		
p_o	180	MeV/c
ε_T	0	mm mr
B_S	3.5	T
B_D	1.3	T
λ_L	1.077	m
L_{BS}	3.231	m

There are no correlations in this 0-emittance initial beam.

Figure 1(a) shows the transverse position in the bend plane (x) as a function of longitudinal position inside a bent solenoid 3 λ_L long. Coordinates are shown for 5 incident momentum centered on the reference momentum p_o. We use a uniform dipole field (no quadrupole component). We see that *x* makes roughly 3 oscillations, but that the period grows as a function of momentum as expected by Eq. 1. These oscillations can be reduced by shaping the dipole field profile at the magnet ends in a second order treatment [4,8]. By the time we reach 2 λ_L the orbits for different momentum are badly spread out, implying that a beam would suffer significant emittance growth. At a distance of 1 λ_L the size of the beam and its *x* divergence is minimal.

Figure 1(b) shows the transverse position in the non-bend plane (y) as a function of longitudinal position inside a bent solenoid 3 λ_L long. Coordinates are shown for 5 incident momentum centered on the reference momentum p_o. We see the spread in vertical position depending on momentum expected from dispersion. The vertical spread continues to build up over all three λ_L. We see that *y* also makes roughly 3 oscillations, each consisting of a fast rise followed by a plateau. At a distance of 1 λ_L the *y* divergence is also minimal.

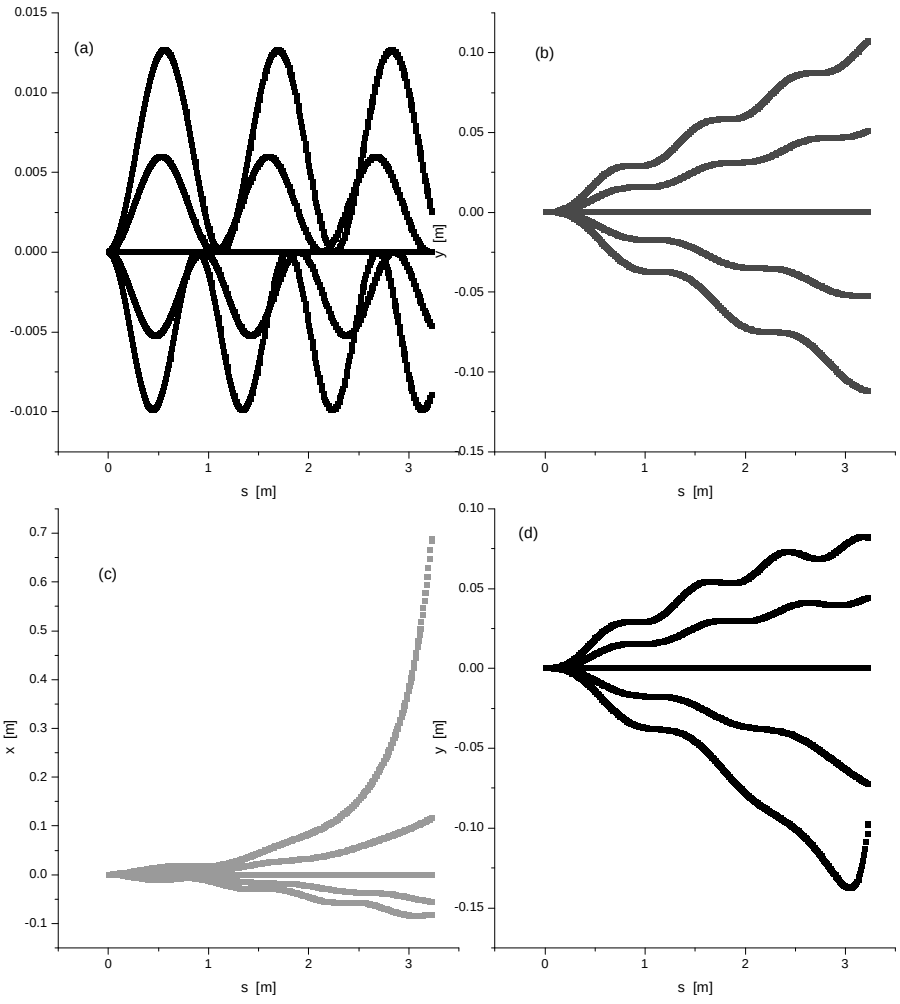

Figure 1. Particle orbits inside the bent solenoid field for particle at 162, 171, 180, 189 and 198 MeV/c. (a) x *vs* s for uniform dipole field; (b) y *vs* s for uniform dipole field; (c) x *vs* s for field with quad component; (d) y *vs* s for field with quad component.

One question that has been raised [4,6,8] is whether the dipole field should be uniform in the radial (x) direction, as it was in Figs. 1(a) and (b), or whether it should vary radially in the same manner as B_S does in Eq. 9. Thus we have set

$$q_Q = -\frac{e}{p_o} b_D^2 \qquad \textbf{(11)}$$

which is -2.81 T/m for the example above. Fig. 1(c) shows that the *x* component of the trajectory. There are similar oscillations over the first λ_L, then the trajectories spread out very rapidly for longer longitudinal path lengths. The *y* trajectories shown in Fig. 1(d) shows the same fast rise and plateau over the first λ_L, but becomes very non-uniform for distances ~3 λ_L.

Further Research - What effect does the quad field have on the transport of a finite emittance beam? Is this the optimal choice of gradient?

From the above considerations we decided to constrain the length of thick bent solenoid elements to be 1 λ_L.

Figure 2(b) shows the dispersion in the direction perpendicular to the bending plane of the bent solenoid. The dispersion curve is fairly (but not exactly) linear. The observed dispersion is ~32 cm, whereas application of Eq. 8 would predict a value of 40 cm. Figure 2(d) shows that the *y* dispersion with the quadrupole component present is practically identical to the uniform dipole case, but has slightly more curvature.

Figure 2(a) shows the dispersion in the bending plane for a uniform dipole field. There is a small, non-linear dispersion for low momentum particles. The peak magnitude of the *x* dispersion is about 10% of the *y* dispersion. The *x* dispersion for the case when the quadrupole component is present is shown in Fig. 2(c). The *x* dispersion is much more linear in this case, and the peak magnitude is ~50% of the *y* dispersion. This means the peak dispersion direction is not aligned with the *y* axis.

It is possible by rotating the coordinate system at the exit of the bent solenoid to eliminate the x dispersion. For the quadrupole example here the true dispersion direction makes an angle of 25° with respect to the y axis. Along this direction the observed dispersion is ~38 cm.

Further Research - Compare this orbit behavior with that expected from a matrix formulation [7]. Can the matrix description be improved? Is it possible to modify Eq. 8 to compute the expected x and y components of the dispersion? How is the expected dispersion influenced by a finite initial emittance? What effect do initial correlations in the beam have?

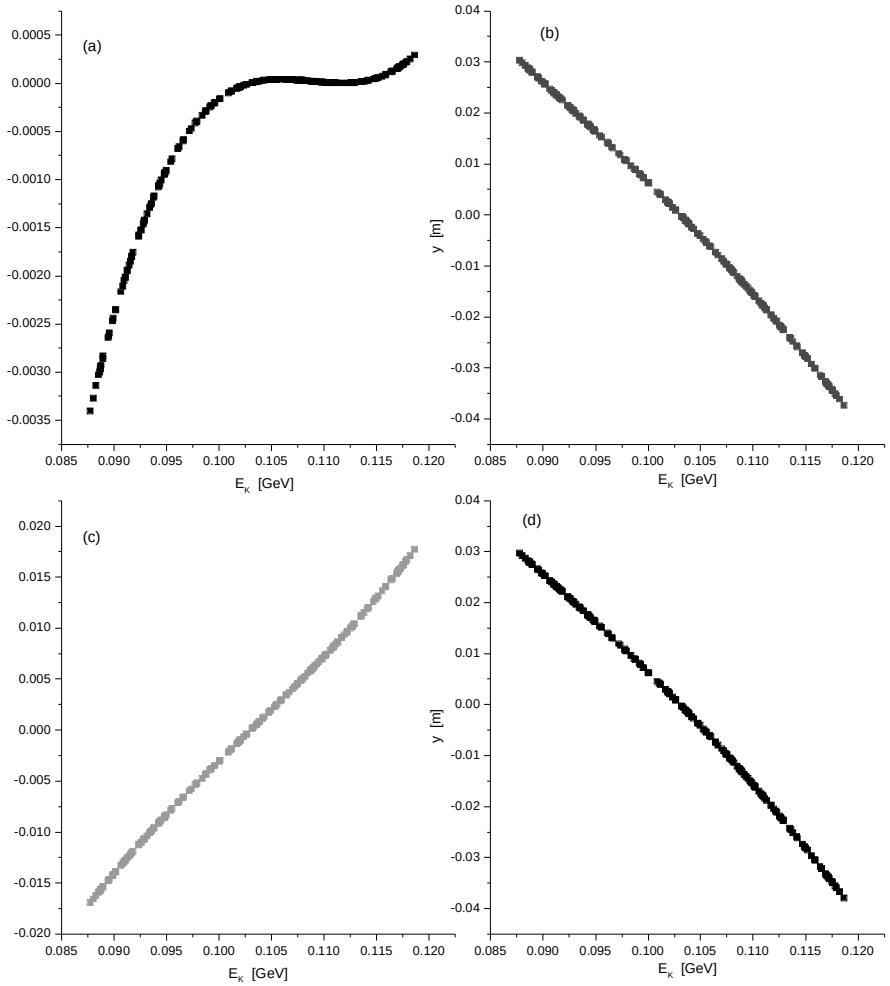

Figure 2. Dispersion for particles uniformly distributed between 162 and 198 MeV/c. (a) x dispersion for uniform dipole field; (b) y dispersion for uniform dipole field; (c) x dispersion for field with quad component; (d) y dispersion for field with quad component.

Figure 3 shows the angular dispersion after a distance of 1 λ_L . Figures 3(a) and (c) show that the *x* angular dispersion is more linear, but larger with the quadrupole component present. The *y* angular dispersions shown in Figs. 3(b) and (d) are very similar and non-uniform in the two cases.

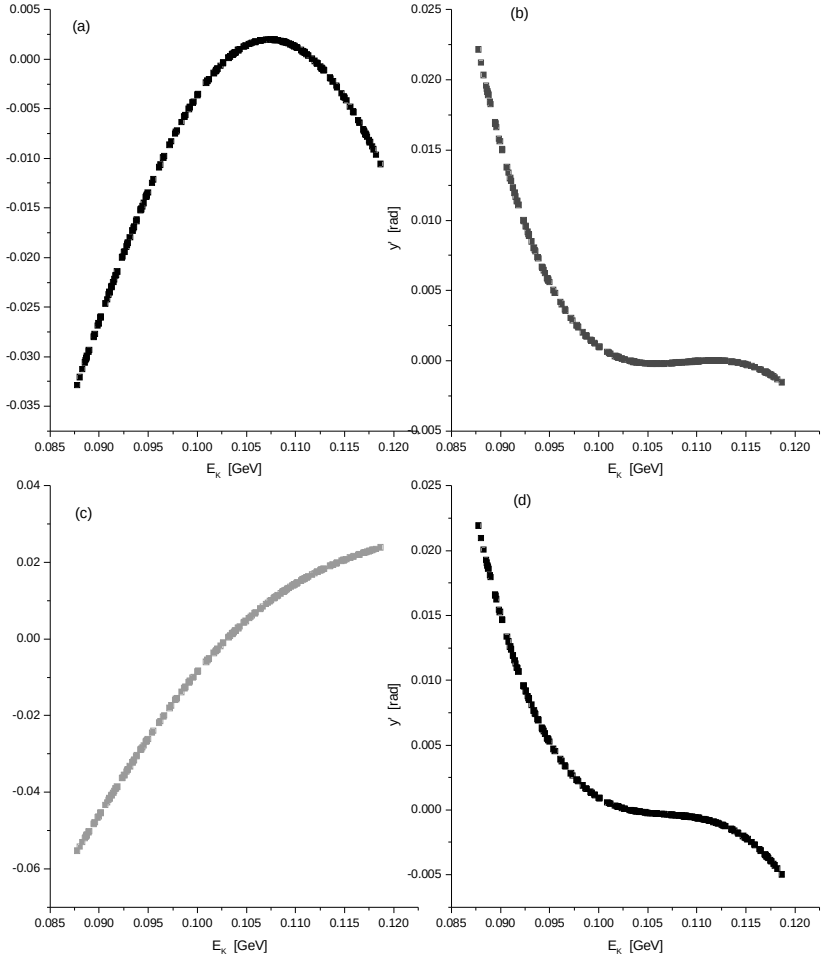

Figure 3. Angular dispersion for particles uniformly distributed between 162 and 198 MeV/c. (a) x' dispersion for uniform dipole field; (b) y' dispersion for uniform dipole field; (c) x' dispersion for field with quad component; (d) y' dispersion for field with quad component.

3.2 Wedge design

The momentum spread in the beam can be removed by following the bent solenoid with a wedge-shaped absorber. For simplicity we use straight edged wedges.

Further Research - Do curved-edged wedges offer any advantages in performance? What is the optimum surface shape?

In general it is preferable to use a number of thin wedges spaced along 1 λ_L, rather than use a single thick wedge [1,4]. Referring to Fig. 4 we see that the wedge dimensions can be approximately determined from the following design equations.

$$\begin{aligned} L_o &= \frac{f\,\Gamma}{n\left\langle \frac{dE}{dz} \right\rangle} \\ w &= 2\,D\,\frac{\Gamma}{p_o} \\ h &= \pm 4\,\sigma_{ND} \\ \tan\frac{\alpha}{2} &= \frac{L_o}{w} \\ L_2 &= 2\,w\,\tan\frac{\alpha}{2} \le L_{region} \end{aligned} \qquad \textbf{(12)}$$

where f is the fraction of the momentum spread we want to remove, Γ is the full half-width of the momentum spread, n is the number of thin wedges we are using, <dE/dz> is the average energy loss in the wedge material, D is the dispersion, w is the width along the dispersion direction, h is the width in the direction perpendicular to the dispersion, and α is the full vertex angle.

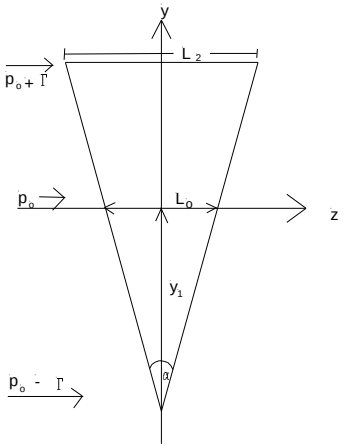

Figure 4. Linear wedge dimensions.

3.3 RF cavity design

We use pillbox *rf* cavities in the TM010 mode. The adjustable parameters are the frequency, cell length, number of cells, peak electric field gradient and cavity phase with respect to a reference particle. Anticipating the actual beam study in the following section, we select an *rf* frequency of 400 MHz. We adopt an upper limit for the field gradient parameter space of 2 Kilpatricks, which is 38 MV/m.

Further Research - How is the exchange performance affected by choosing a different frequency or different cavity model?

3.4 System configuration

The beam passing thru the bent solenoid and wedge develops a number of strong correlations. There is a negative correlation between p_z and t due to the fact that slower momentum particles take longer to get thru the system. This is a particular concern for systems with thick elements since the beam has to go long distances between *rf* cavities. Then because of the dispersion there are also strong correlations between *y* and *t* and between *y* and p_z.

Further research - How is the exchange performance affected by the initial correlation of momentum and transverse amplitude? How is it affected by the shape of the initial longitudinal phase space?

The simplest arrangement of components into an exchange system would seem to have the following configuration

BS(y) - W(y) - RF1 - BS(x) - W(x) - RF2

where BS(y) means a bent solenoid that produces dispersion primarily along y, etc. The *rf* systems are used to restore the beam to its initial conditions and orientations, apart from the momentum spread and transverse beam size. We have been unsuccessful [9] in trying to design a simple system of this type.

We also investigated [9] a (half) system with the configuration

RF1 - BS(y) - W(y) - RF2 - ...

where we tried to use the first *rf* cavity (RF1) to make a positive slope in (t, p_z) . We were successful in getting a slope that balanced the effect of the bent solenoid, but could not simultaneously obtain an average kinetic energy that matched the bent solenoid design value.

Thus we were lead to the more complicated (half) system [9] suggested by R. Palmer

BS1(y) - RF1 - BS2(y) - W(y) - RF2 - ...

The idea is to break up the bent solenoid region into two symmetric halves and to put an *rf* cavity (RF1) in between them. The cavity is used to reverse the slope of (t, p_Z), so that when the beam reaches the wedges the longitudinal correlation has been removed. By reversing the dipole direction in the second half bent solenoid, the dispersions should add while the aberrations should cancel. Thus the design requirements[2] on RF1 are:

1. σ_t should be conserved
2. r (t, p_Z) --> -r (t, p_Z)
3. <KE> should be conserved
4. keep σ_E ~ initial value

at the end of BS2.

The second *rf* cavity should restore the mean beam energy and phase space orientations so that a subsequent system could work in a similar manner with dispersion in the *x* direction. Thus the design requirements on RF2 are:

1. restore <KE> to reference value
2. keep $\sigma_E \leq$ value after wedge
3. r (t, p_Z) ~ 0
4. r (x, p_Z) ~ 0
5. r (y, p_Z) ~ 0

at the midpoint of the exchange system.

Further Research - Can we use a beam optics code to examine possible exchange configurations? Is the configuration given here the optimum one?

3.5 Second order fields

The second order analytic fields in a dipole-compensated bent solenoid are considerably more complicated than Eqs. 9 and 10. The dipole has the following field components.

$$\begin{aligned} B_X(x,y,s) &= a_{11}(s)\,y + a_{12}(s)\,x\,y \\ B_Y(x,y,s) &= a_{10}(s) + a_{11}(s)\,x + \frac{1}{2}a_{12}(s)\,x^2 + \frac{1}{2}a_{30}(s)\,y^2 \\ B_S(x,y,s) &= a_{10}'(s)\,y + (a_{11}'(s) - h(s)\,a_{10}'(s))\,x\,y \end{aligned} \qquad \textbf{(13)}$$

[2] r (a,b) refers to the linear correlation coefficient between the variables a and b. The quantity r has the value 1 (-1) for perfect correlation with positive (negative) slope, while r=0 for an uncorrelated (upright) distribution.

where primes refer to derivatives with respect to s. The quantity a_{10} is the dipole field on axis and a_{11} is the quadrupole gradient on axis. These can be specified arbitrarily. The form used in the program ICOOL is

$$\begin{aligned} a_{10}(s) &= b_D\ \Delta\tanh(s; c_D, e_D, \lambda_D) \\ a_{11}(s) &= g_Q\ \Delta\tanh(s; c_Q, e_Q, \lambda_Q) \end{aligned} \qquad \textbf{(14)}$$

where Δtanh is the difference of two hyperbolic tangent functions of *s* with parameters *c* specifying the central length, *e* specifying the *s* offset at the end, and λ specifying how rapidly the field decays at the ends. The curvature of the bent solenoid follows that generated by the dipole and is given by

$$h(s) = \frac{q}{p_o} B_Y(0,0,s) \qquad \textbf{(15)}$$

The sextupole components a_{12} and a_{30} in the dipole field above are not independent in second order. According to Maxwell's equations they must satisfy the constraints

$$\begin{aligned} a_{12}(s) &= 2a_{10}'' + a_{11}h - \frac{1}{h}a_{11}'' + a_{10}'\frac{h'}{h} \\ a_{30}(s) &= -a_{12} - a_{11}h - a_{10}'' \end{aligned} \qquad \textbf{(16)}$$

The bent solenoid itself requires the superposition of the field components

$$\begin{aligned} B_X(x,y,s) &= -\frac{1}{2}\left(B_{so}'(s)\,x - \frac{1}{2}B_{so}(s)\,h'(s)\,x^2 - \frac{3}{2}B_{so}'(s)\,h(s)\,x^2 \right) \\ B_Y(x,y,s) &= -\frac{1}{2}\left(B_{so}'(s)\,y - 2B_{so}'(s)\,h(s)\,x\,y - B_{so}(s)\,h'(s)\,x\,y \right) \\ B_S(x,y,s) &= \left(1 - h(s)\,x + h^2(s)\,x^2\right) B_{so}(s) \end{aligned} \qquad \textbf{(17)}$$

There is a third independent function B_{so} giving the solenoid field on axis.

$$B_{so}(s) = b_S\ \Delta\tanh(s; c_S, e_S, \lambda_S) \qquad \textbf{(18)}$$

Further Research - Examine the effect of different coupling schemes into the bent solenoid [1,4,8]. Is the Δtanh shape satisfactory to represent the end fields? How does the coupling configuration depend on the initial beam conditions? What constraints are necessary for proper matching?

4 Emittance exchange system design

We now consider the design of an actual emittance exchange system. The first half, dealing with dispersion in y, is shown schematically in Fig. 5.

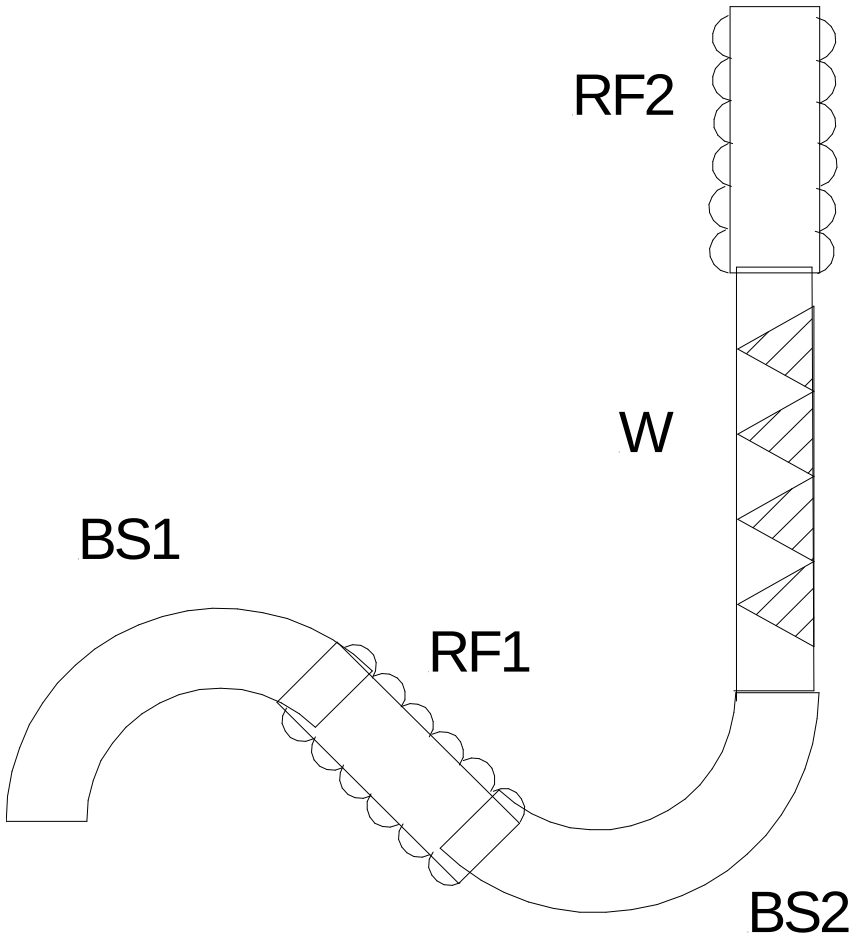

Figure 5. Schematic layout of one half of an emittance exchange system.

The input beam parameters are given in Table 2.

Table 2 Beam parameters[3]			
	Entrance	Exit	
p_o	180	180	MeV/c
σ_X	21.1	19.1	mm
σ_Y	21.2	36.4	mm
σ_Z	20	68	mm
σ_{Px}	14.9	13.8	MeV/c
σ_{Py}	15.6	14.2	MeV/c
σ_{PZ}	9.2	7.1	MeV/c
ε_{TN}	2.08	2.79	mm
ε_{LN}	1.68	2.17	mm
ε_{6N}	71	148	x 10^{-10} m^3

The input beam was given the angular momentum correlation appropriate for motion in a 3.5 T solenoidal field.

Further Research - Investigate the exchange performance over the muon collider range of parameters specified in Fig. 23 of the Status Report [1].

The design parameters for the bent solenoids are given in Table 3. The total length was 2 λ_L. The fields were described using the second order equations in section 3.5. The solenoid field is constant. The dipole field has the shape shown in Fig. 6. The bend angle is 143° and the radius of curvature is 50 cm. We adopted a maximum limit of 180° on the bend angle and a minimum limit of 50 cm for the radius of curvature. The design of BS1 and BS2 only differ in the direction of the dipole field.

Further Research - What are the practical limits on the bend angle and radius of curvature?

[3] We are using emittance definitions using the covariance matrix, so all second order off-diagonal correlations have been removed.

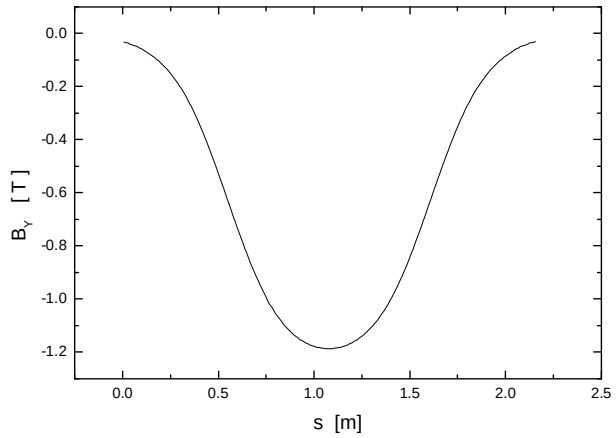

Figure 6. Dipole field profile for BS1.

Table 3 Bent solenoid parameters		
B_S	3.5	T
B_D (peak)	±1.19	T
g_Q	0.	T / m
L	2.16	m
θ	143	deg
ρ	0.5	m
c_D	1.06	m
e_D	0.55	m
λ_D	0.3	m

A constant solenoid field has an associated beta function

$$\beta_{\perp} = \frac{2\,p_Z}{e\,B_S} \qquad \textbf{(19)}$$

which should be matched to the initial transverse phase space.

The system performance is summarized in Tables 2 and 6. The bent solenoid generates significant correlations, as expected. The produced dispersion can be computed numerically from

$$D = \frac{\sqrt{\sigma_{y1}^2 - \sigma_{y0}^2}}{\frac{\sigma_P}{p_o}} \qquad \textbf{(20)}$$

where {0,1} refers to values at the {entrance, exit} of the bent solenoid. We find that D_Y = 34.4 cm and D_X = 0. cm.

Further Research - Does higher dispersion offer any advantage? Does lower dispersion reduce the phase space distortions?

The design parameters for RF1 are given in Table 4. We fixed the frequency, number of cells, and cell length. The total length was 2 λ_L. The gradient and phase offset was assumed to be the same in all 13 cells. That leaves two adjustable parameters, the magnitude of the gradient and the phase offset[4]. We used these to (1) keep the mean energy of the bunch constant and (2) require an upright longitudinal phase space ellipse at the end of the second half of the bent solenoid (BS2). The dependence of various quantities as a function of phase is shown in Fig. 7.

[4] ICOOL defines 0° phase to correspond to the reference particle crossing the center of the cavity at 0-crossing of the electric field.

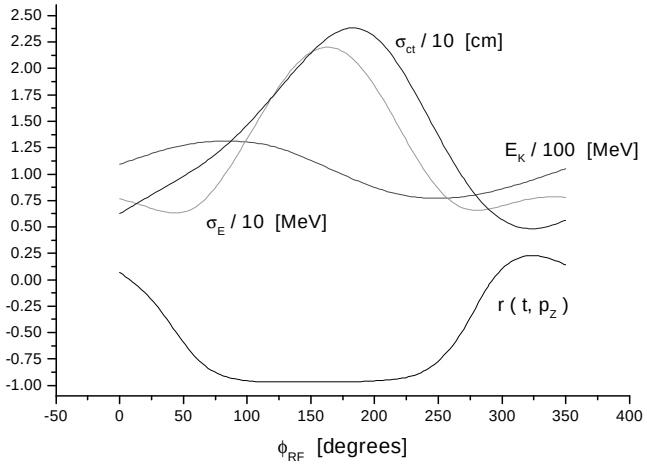

Figure 7. Dependence of average kinetic energy, energy spread, bunch length, and longitudinal phase space correlation on phase for RF1. The gradient is 17 MV/m.

Table 4 RF system design parameter			
RF1	f	400	MHz
	G	17	MV / m
	φ	-14	deg
	N_{cells}	13	
	L_{cell}	16.62	cm
RF2	f	400	MHz
	G	12	MV / m
	φ	24	deg
	N_{cells}	13	
	L_{cell}	16.62	cm

Further Research - Doing this two parameter optimization by hand is slow and tedious. Is there any theoretical guidance on how to set these parameters? Can we develop an RF optimizer inside ICOOL (or its equivalent) ? What is the effect on the performance of adding Be end windows to the rf cavities?

BS2 is identical to BS1 except for reversing the direction of the dipole field. At the end of BS2 the dispersion D_Y = 61.4 cm and D_X = 0. cm, ignoring any emittance growth in RF1. Thus we see that the dispersion does in fact add to that produced in BS1.

Further Research - Why don't the dispersion in BS1 and BS2 add linearly? Examine claims that the aberrations cancel in this configuration.

Figure 8 shows the evolution of longitudinal phase space from production, after BS1, after RF1 and after BS2. In Fig. 8(b) we see the expected negative correlation from lower momentum particles taking longer to get thru BS1. RF1 makes the desired change in slope, as shown in Fig. 8(c). Finally the result of going thru the symmetric BS2 is shown in Fig. 8(d). The distribution ends up approximately upright before going into the wedges, but the resulting distribution is clearly distorted compared to the initial beam in Fig. 8(a).

The corresponding change in the dispersion from production to BS2 is shown in Fig. 9. One clearly sees the dispersion produced in BS1 in Fig. 9(b). Figure 9(c) shows that there is no apparent dispersion following RF1. However, Fig. 9(d) shows the increase in dispersion after BS2.

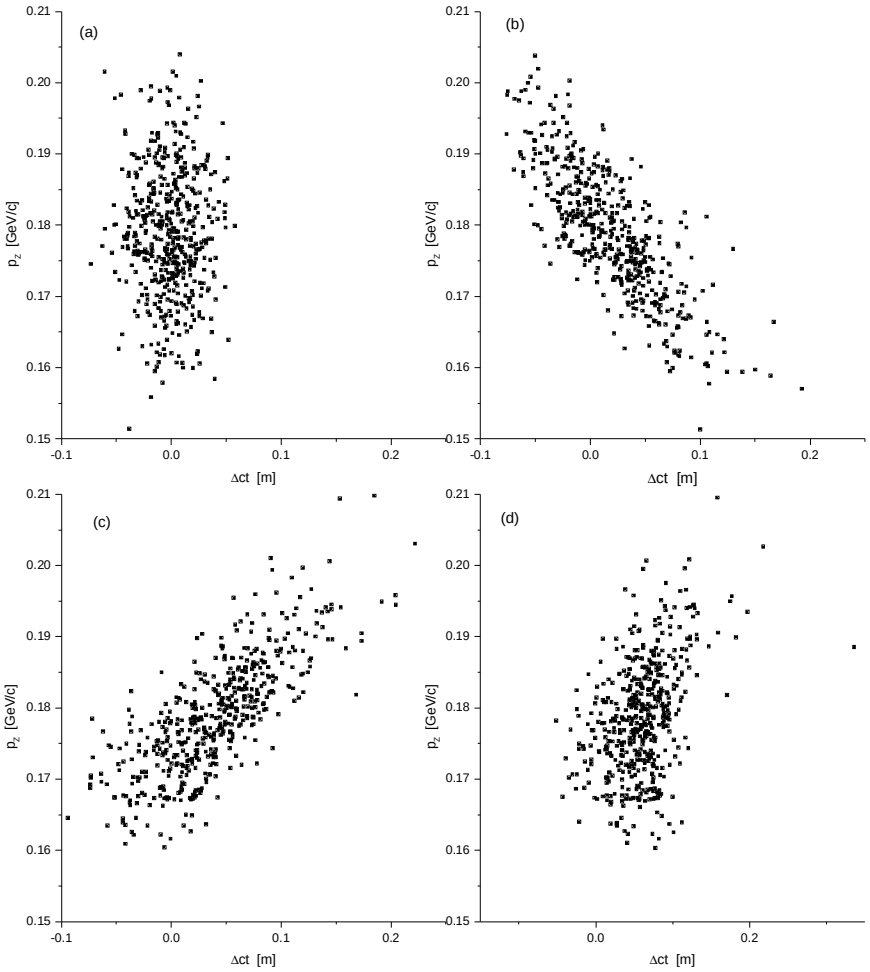

Figure 8. Longitudinal phase space distribution, p_Z *vs* ct (a) at production; (b) after BS1; (c) after RF1; (d) after BS2.

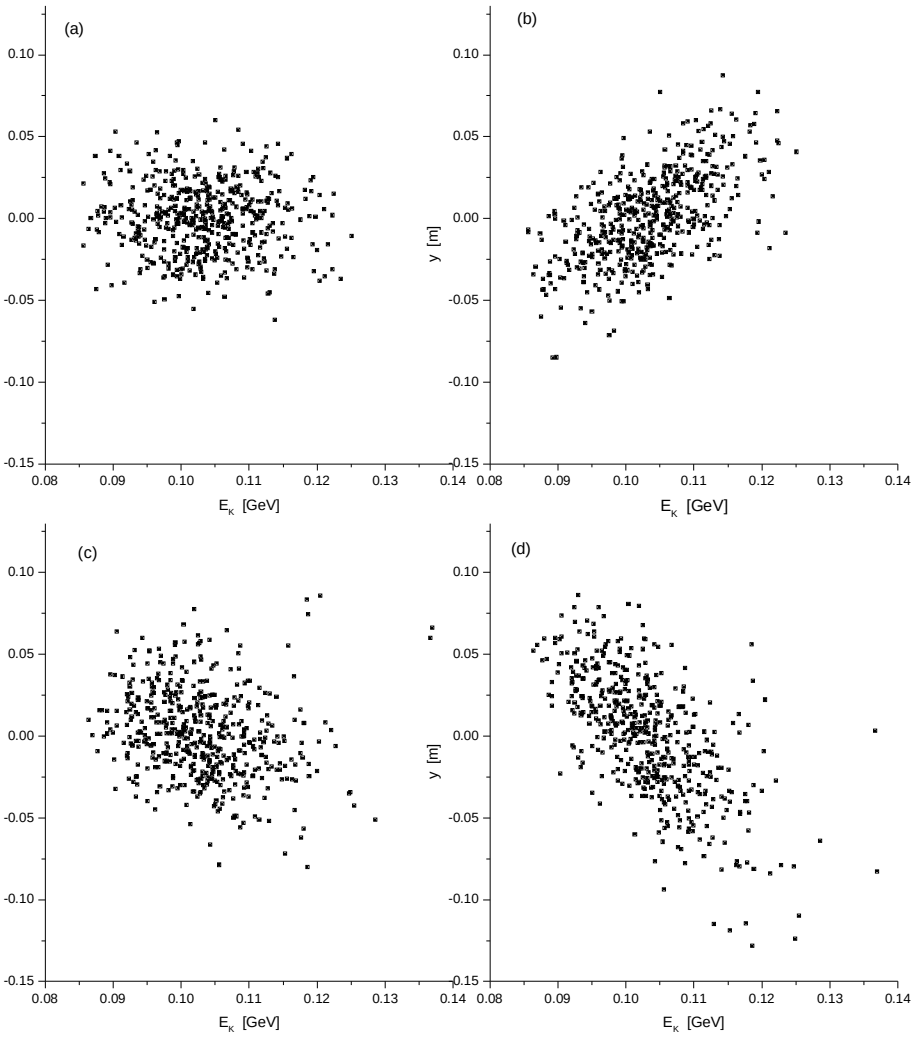

Figure 9. Dispersion distribution, y *vs* E_K (a) at production; (b) after BS1; (c) after RF1; (d) after BS2.

The design parameters for the wedges are given in Table 5. The wedges were designed to remove the *y* dispersion from the beam. Four wedges were equally spaced over 1 λ_L. The procedure used was to first set the azimuthal angles φ for all the wedges such that the wide side of the wedge matched the high energy side of the beam. Then the opening angles α of all the wedges were adjusted simultaneously to minimize the energy spread and *y* dispersion at the end. We then searched for evidence of a dispersion wave by adjusting the azimuthal angle of each wedge individually. The dispersion wave correction was very small, only reducing the energy spread given in Table 6 by less than 1%. The change in dispersion going thru each of the four wedges is shown in Fig. 10. The slope in the dispersion distribution is removed incrementally, leading finally to an upright ellipse.

Further Research - What theoretical justification is there for a dispersion wave? At what rate do we expect to have to rotate the wedges? How much improvement in energy spread reduction do we expect over using wedges at a fixed azimuthal angle?

The ability of the wedges to decrease the energy spread diminishes quickly. The energy spread of 7.83 MeV after BS2 drops to 7.20, 6.75, 6.45, and 6.47 MeV in passing thru the four LiH wedges.

Further Research - How much better could we do with liquid hydrogen wedges? How practical is a liquid hydrogen "wedge"?

Table 5 Wedge design parameters

material	LiH	
N_{wedges}	4	
L_{region}	27	cm
α	13	deg
φ	90	deg
w	22	cm
h	22	cm

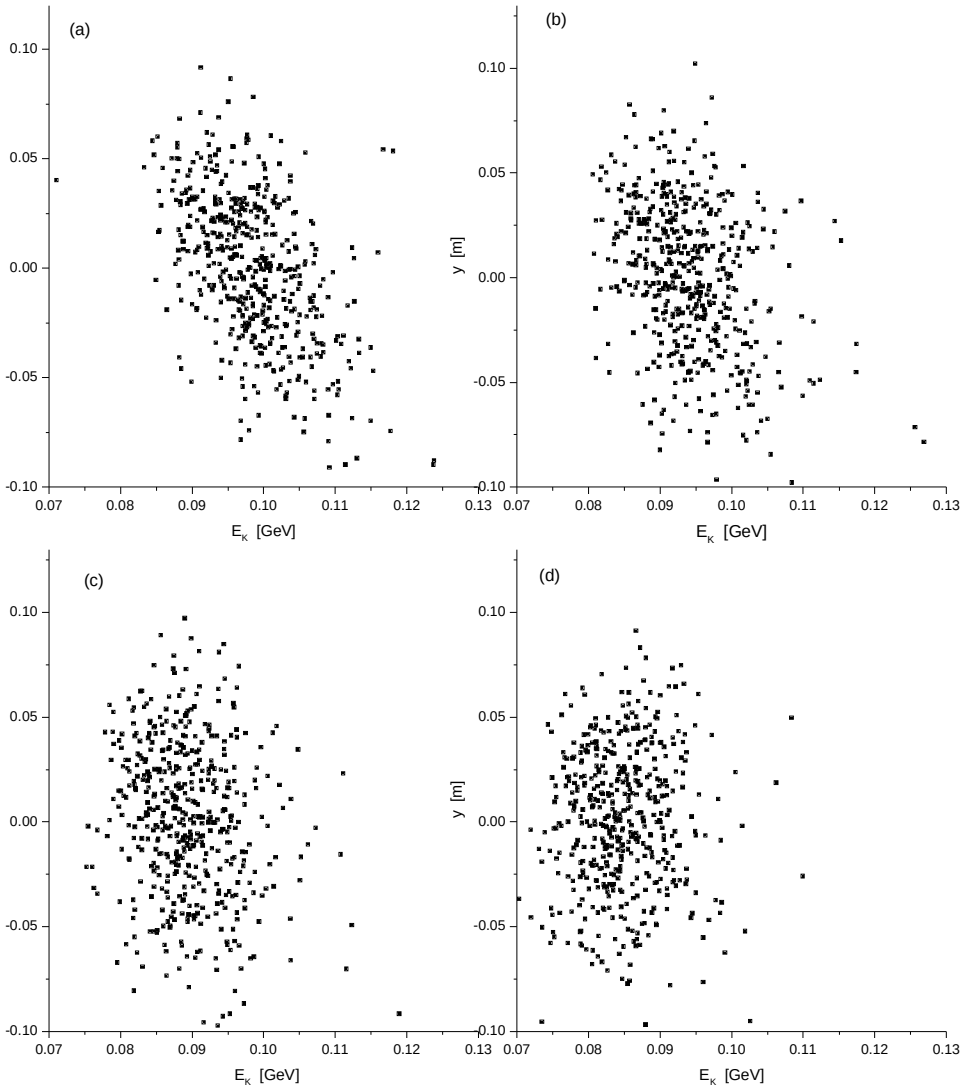

Figure 10. Dispersion distribution, y *vs* E_K (a) after wedge 1; (b) after wedge 2; (c) after wedge 3; (d) after wedge 4.

The design parameters for RF2 are also given in Table 4. We fixed the frequency, number of cells, and cell length. The total length was 2 λ_L. The gradient and phase offset was assumed to be the same in all 13 cells. That leaves two adjustable parameters, the magnitude of the gradient and the phase offset. We used these to (1) make up for the energy lost in the wedges and restore the mean energy of the bunch to its initial value and (2) require an upright longitudinal phase space ellipse at the end of the half emittance exchange system (midpoint of a complete exchange system). The performance values given in Tables 2 and 6 shows that this optimization was not successful. The longitudinal phase space is seriously distorted and there is significant apparent dispersion remaining in the beam. It is possible that we are way off from the correct gradient and phase values or, more likely, that a more complicated *rf* arrangement is necessary to accomplish what we want.

Further Research - Is there any theoretical guidance on how to set these parameters? Do we need more adjustable parameters? Can we control the pulse distortion by adding higher harmonic cavities?

Table 6 System performance

	Start	BS1	RF1	BS2	WED	RF2
<KE> [MeV]	103.2	103.2	103.1	103.1	84.9	103.3
σ_{KE} [MeV]	7.76	7.76	7.83	7.83	6.47	6.44
σ_{ct} [cm]	2.3	4.6	5.7	5.4	5.9	8.1
r (x, KE)	-0.03	0.01	0.02	0.01	0.21	0.19
r (y, KE)	-0.02	0.60	-0.17	-0.65	-0.09	-0.28
r (t, p_Z)	-0.04	-0.80	0.58	0.17	-0.29	-0.44

The total length of the half exchange system is 9 λ_L = 9.72 m. The transmission is 0.988.

The longitudinal phase space at the end of the half system is shown in Fig. 11. This distribution is badly distorted compared with the distribution entering the first half of the system shown in Fig. 8(a). Thus there is little point going on to consider the second half of the system, since one would expect its performance will be even worse than the part already discussed.

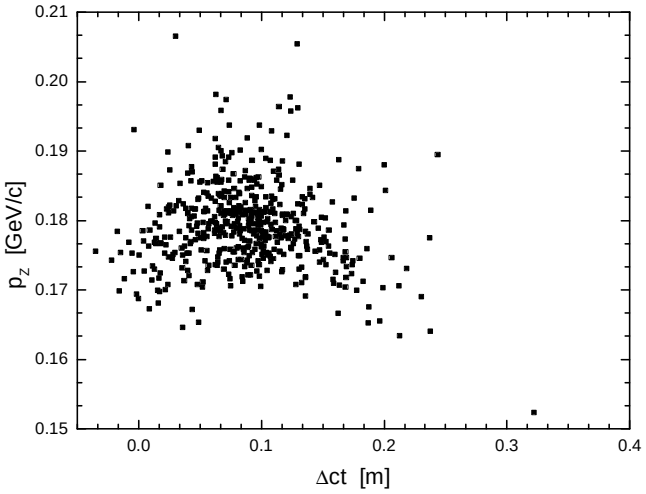

Figure 11. Longitudinal phase space distribution at the end of the (half) emittance exchange system.

5 Conclusions

We have been unable to find a satisfactory solution to the design a 6-dimensional emittance exchange system using thick bent solenoid elements. Although the energy spread was reduced, the longitudinal and 6-D emittances increased substantially getting thru this system. A clean input beam quickly develops correlations in the bent solenoid that cause severe phase space distortions in the *rf* cavity fields. Of course the development of the design discussed here involved making many choices of configuration and parameter values, so these results do not indicate that a solution is not possible. Indeed, we have identified many areas where further work could lead to improvements. However, it's clear that theoretical guidance would be very valuable for further investigations of complicated systems like this.

Acknowledgments

We would like to thank Bob Palmer, Jim Norem and Gail Hanson for useful discussions.

Notes and references

[1] C. Ankenbrandt et al, Status of muon collider research and development and future plans, Phys. Rev. ST-AB 2:081001-1-73, 1999, p. 27-32.
[2] D. Neuffer, Phase space exchange in thick wedge absorbers for ionization cooling, in D. Cline (ed), Physics Potential and Development of $\mu^+\mu^-$ Colliders, AIP Conf. Proc. 441, 1998, p.

270-281.
[3] J. Gallardo, R. Fernow & R. Palmer, Muon dynamics in a toroidal sector magnet, in D. Cline (ed), Physics Potential and Development of $\mu^+\mu^-$ Colliders, AIP Conf. Proc. 441, 1998, p. 282-288.
[4] J. Norem, Coupling sections, emittance growth, and drift compensation in the use of bent solenoids as beam transport elements, Phys. Rev. ST-AB 2:054001-1-10, 1999.
[5] F. Chen, Introduction to Plasma Physics, Plenum Press, 1979, p. 23-26.
[6] C. Lu, K. McDonald, E. Prebys & S. Vahsen, A detector scenario for the muon cooling experiment, unpublished Princeton University report μμ/97-8, revised May 15, 1998, p. 10-13.
[7] J. Gallardo, Transfer matrix for combined dipole + bent solenoid, Mucool Note 15, 1999.
[8] R. Palmer, Emittance Exchange & Full System, in Particle Accelerator School notes, Vanderbilt University, 1999,
http://pubweb.bnl.gov/people/palmer/course/9exch.ps
[9] R. Fernow, Emittance exchange studies with RF, presented at FNAL Cooling Workshop, 7 December 1998.